

the use of Heiniger's¹¹ method for estimating the electronic contribution to the specific heat of chromium. Nevertheless, close to the Néel temperature, there exists a discrepancy (between theory and experiment) as to the shape of the C_p curve which does not appear to be accounted for by reasonable changes in the parameters used in determining C_p . However, in view of the numerous physical assumptions implied by the models used, this discrepancy is not surprising. For example, the electronic model corresponds to a second-order phase transition at T_N , whereas it is known that the transition is first order.³¹ Also, effects of a possible temperature dependence of the frequency spectrum due to changes in the electronic structure have been ignored

³¹ S. A. Werner, A. Arrott, and H. Kendrick, Phys. Rev. **155**, 528 (1967).

in our lattice model. Such effects in the long-wavelength part of the spectrum seem apparent from the elastic constant data.

ACKNOWLEDGMENTS

The author thanks Dr. J. de Launay, Dr. J. L. Katz, and Dr. E. F. Skelton for their interest in this work and for many helpful discussions regarding it, and Dr. T. M. Rice and Dr. H. B. Rosenstock for valuable conversations. Dr. L. C. Towle's reading of the manuscript and helpful suggestions are appreciated. Dr. S. K. Sinha and Dr. G. Gilat are thanked for sending their results before publication, and Dr. J. S. Brown's sending of a frequency-spectrum computer program is acknowledged.

¹¹⁵In NMR in the Indium-Rich Alloys In-Cd, In-Hg, and In-Tl at 4.2°K*

F. C. THATCHER† AND R. R. HEWITT

Department of Physics, University of California, Riverside, California 92502

(Received 17 June 1969; revised manuscript received 24 September 1969)

Nuclear magnetic resonance has been observed in the indium-rich alloys In-Cd, In-Hg, and In-Tl at 4.2°K. Measurements have been made of the isotropic Knight shift, anisotropic Knight shift, quadrupole-coupling frequency, and linewidths as a function of solute concentration to 4.7 at.% Cd, 4.3 at.% Hg, and 7.9 at.% Tl. The isotropic Knight shift exhibits a dip similar to that previously observed in In-Sn and In-Pb. The sign of the electric field gradient has been deduced from the quadrupole-coupling frequencies in the alloys, and is negative. The screening theory of Kohn and Vosko is found to describe line broadening in these indium alloys, and the enhancement factor of that theory is determined to be 85 ± 15 .

I. INTRODUCTION

IT is possible, in indium metal and its alloys, to obtain the Knight shifts and the electric quadrupolar coupling between indium nuclei and their environment by nuclear-magnetic-resonance measurements. The angular dependence of the anisotropic Knight shift allows its separation from the isotropic Knight shift, while the m dependence of the quadrupolar perturbation allows its separation from the m -independent Knight shifts. In practice, our measurements are made on metal powders and at a fixed field. Certain difficulties arise in the interpretation of broadened powder-pattern resonance lines. These have been discussed for pure indium by Adams *et al.*¹

The introduction of substitutional impurities results in long-range screening of the impurities by the conduction electrons.²⁻⁴ This screening produces shifts in

the mean or peak absorption frequencies and, in general, asymmetric broadening of the resonance lines. Such broadening and shifts raise questions concerning the measurement and interpretation of resonance lines exhibiting these effects. We shall attempt to clarify the problem by examining the linewidths and line shapes in indium alloys.

In the presence of quadrupole interactions, the addition of a few atomic percent of impurities can easily result in the doubling of the linewidth, providing a good quantitative test of the theories. In this work, we employ the screening theory of Kohn and Vosko,⁴ which takes into account the fact that screening electrons are Bloch electrons rather than free electrons, and show how the enhancement factor of the theory can be obtained from the width data. The enhancement factor provides an interesting test of electronic wave functions in a metal, and is necessary for the calculation of line shapes and the contribution of screening to the

* Work supported by the National Science Foundation.

† Present address: California State College, San Bernardino, Calif.

¹ J. E. Adams, B. F. Williams, and R. R. Hewitt, Phys. Rev. **151**, 238 (1966).

² J. Friedel, Nuovo Cimento Suppl. **7**, 299 (1958).

³ A. Blandin and E. Daniel, J. Phys. Chem. Solids **10**, 126 (1959).

⁴ W. Kohn and S. H. Vosko, Phys. Rev. **119**, 912 (1960).

anisotropic Knight shift and quadrupolar interactions in alloys.

This work was initiated with a number of goals in mind. Providing more information about the sharp drop in the isotropic Knight shift, observed in the indium-lead and indium-tin alloys at low concentrations,⁵ was high among these. The need to eliminate the possibility that the drop in the Knight shift was due to an interpretational error motivated our line-shape investigation. Additional information concerning the nuclear quadrupole interaction was also desirable, as conclusions based on only two alloy systems (In-Sn and In-Pb) were tentative.

Measurements are reported here of the ¹¹⁵In isotropic Knight shift K , the anisotropic Knight shift a , and the quadrupole-coupling frequency ν_q , as a function of solute concentration in the indium-rich solid solutions In-Cd, In-Hg, and In-Tl, at 4.2°K. Linewidth data for these systems and for In-Sn and In-Pb are also presented. Experimental details are discussed in Sec. II. Theoretical expressions for screening contributions to the resonance shifts and broadening are presented in Sec. III along with linewidth results and line-shape calculations. Knight shift and quadrupole-coupling results are given in Sec. IV and are discussed in terms of the screening theory of Kohn and Vosko⁴ and in the light of recent work on the effects of electron-electron interactions on Knight shifts.^{6,7} Our conclusions are summarized in Sec. V.

II. EXPERIMENTAL

All alloys were obtained from the Indium Corp. of America, the In-Cd and In-Tl alloys in the form of 325 mesh powder and the In-Hg alloys in the form of ingots. Spectroscopic trace analyses were run on all powdered samples and only negligible traces of other impurities were measured. In-Hg powders were prepared by sonorating the ingots in decane using an induction heater to melt the ingots.

All measurements were made at 4.2°K with a marginal oscillator, similar to the Pound-Knight oscillator,⁸ with frequency-sweep and phase-sensitive detection. The measurements were made in an applied magnetic field of 27.3 kG. Field measurements were obtained by measuring the ⁶³Cu resonance in a copper powder sample placed in the center of the indium alloy sample.

The resonance frequencies in a single crystal are functions of the angle θ between the applied magnetic field and the crystal symmetry axis. In a powder, singularities in power absorption occur whenever the condition $d\nu/d\cos\theta=0$ is fulfilled. Measurements were made of the three most intense singularities. These are the 90° (ν_H) and non-90° (ν_L) singularities correspond-

ing to the $\frac{1}{2} \rightarrow -\frac{1}{2}$ transition and the 90° ($\nu_{3/2}$) singularity of the $\frac{3}{2} \rightarrow \frac{1}{2}$ transition. For pure indium, perturbation expressions for these singularities are^{9,10}

$$\begin{aligned}\nu_H &= \nu_0 - a\nu_R + \frac{3}{2}(\nu_q^2/\nu_0), \\ \nu_L &= \nu_0 + \frac{2}{3}a\nu_R - (8\nu_q^2/3\nu_0) - (a^2\nu_R^2\nu_0/6\nu_q^2), \\ \nu_{3/2} &= \nu_0 - a\nu_R - \frac{1}{2}\nu_q + \frac{21}{16}\frac{\nu_q^2}{\nu_0} + \frac{129}{64}\frac{\nu_q^3}{\nu_0^2},\end{aligned}$$

where

$$\nu_0 = (1+K)\nu_R,$$

and

$$\nu_R = \gamma_n H / 2\pi.$$

It is necessary to include third-order terms in the quadrupole-coupling frequency in order to take full advantage of the experimental precision of 2 kHz for low concentrations. We shall show in Sec. III that these expressions are valid, to a very good approximation, in indium alloys also, as long as the measured quantities are mean frequencies and the Knight shifts and quadrupole coupling are interpreted as mean values averaged over all nuclear sites. The positions of these singularities were obtained from the dipolar-broadened derivative NMR lines according to the prescription of Adams *et al.*,¹ which assumes Gaussian dipolar broadening. Linewidths were obtained in the same way. Asymmetric broadening produced by impurity screening was ignored in the experimental determination of linewidths. The resonance lines in the alloys continued to exhibit the shape characteristic of Gaussian broadening. The validity of this procedure is examined in more detail in Sec. III. The perturbation expressions for the powder-pattern singularities (ν_H , ν_L , and $\nu_{3/2}$) may be solved by iteration for the Knight shifts and quadrupolar coupling. Each singularity was measured three times and errors are given as the standard deviation of the 27 solutions obtained for K , a , and ν_q .

III. IMPURITY SCREENING EFFECTS

We assume that the substitutional impurities in the alloy are distributed at random on lattice sites and that the impurities are independently screened by the conduction electrons. We neglect surface effects. Thus, if $P(\mathbf{R}_j)$ is any quantity, to be evaluated at a nuclear site \mathbf{R}_j , which depends in a linear way on the screening charge density then $P(\mathbf{R}_j)$ may be written

$$P(\mathbf{R}_j) = P_0 + \sum_{i=1}^n \Delta P(\mathbf{R}_{ij}),$$

where the sum is over all impurity sites, $\Delta P(\mathbf{R}_{ij})$ is the change in P due to screening, and P_0 is the value of P in the absence of screening. With these assumptions,

⁵ W. T. Anderson, F. C. Thatcher, and R. R. Hewitt, Phys. Rev. **171**, 541 (1968).

⁶ T. Moriya, J. Phys. Soc. Japan **18**, 516 (1963).

⁷ A. Narath and H. T. Weaver, Phys. Rev. **175**, 373 (1968).

⁸ R. V. Pound and W. D. Knight, Rev. Sci. Instr. **21**, 219 (1950).

⁹ R. G. Barnes, D. J. Ganin, R. G. Lecander, and D. R. Torgeson, Phys. Rev. **145**, 302 (1966).

¹⁰ J. E. Adams, L. Berry, and R. R. Hewitt, Phys. Rev. **143**, 164 (1966).

exact expressions may be written for the mean value and second moment of the distribution of P in the alloy. These are¹¹

$$\bar{P} \equiv \frac{1}{N} \sum_{j=1}^N P(\mathbf{R}_j) = P_0 + c \sum_{\mathbf{R}'} \Delta P(\mathbf{R}), \quad (1)$$

$$\begin{aligned} \langle \delta^2 P \rangle_{\text{av}} &\equiv \frac{1}{N} \sum_{j=1}^N P^2(\mathbf{R}_j) - \bar{P}^2 \\ &= c(1-c) \sum_{\mathbf{R}'} [\Delta P(\mathbf{R})]^2, \end{aligned} \quad (2)$$

where c is the atomic fraction of solute and the sum is over all lattice sites except an origin. Since the Knight shifts and the electric-field-gradient (EFG) tensor components depend linearly on the charge density, these formulas apply to them.

We wish to show that the perturbation expressions given in Sec. II for pure indium apply in a substitutional alloy when all quantities are interpreted as mean values. We can write the perturbation expression for the transition frequencies of a nucleus to first order in the Knight shifts and third order in the quadrupolar interaction. We do not repeat the third-order calculation which has been published elsewhere.¹² For the sake of brevity we examine only the $\frac{1}{2} \rightarrow -\frac{1}{2}$ transition. The third-order term in the quadrupolar interaction vanishes for this transition, and we have

$$\nu(\mathbf{R}_j) = \nu_0 + a_j \nu_R (3\mu^2 - 1) + (8/3) \lambda_j^2 \nu_0 [|V_{+2}^j|^2 - 2 |V_{+1}^j|^2], \quad (3)$$

where

$$\mu = \cos \theta,$$

and

$$\lambda_j = 3eQ/2I(2I-1)\hbar\nu_0.$$

The EFG tensor components are defined in the usual way¹³ and are evaluated in the magnetic field frame of reference. Transforming to a coordinate system whose z axis is taken in the direction of the crystal symmetry axis, the EFG tensor components are⁴

$$\begin{aligned} (V_0^j)' &= eq + \alpha f_0(\mathbf{R}_j) \\ &\equiv eq + \alpha e \sum_{i=1}^n \frac{(3Z_{ij}^2 - R_{ij}^2)}{R_{ij}^2} \Delta q(\mathbf{R}_{ij}), \\ (V_{\pm 1}^j)' &= \alpha f_{\pm 1}(\mathbf{R}_j) \\ &\equiv \alpha e \sum_{i=1}^n \frac{3Z_{ij}(X_{ij} \pm iY_{ij})}{R_{ij}^2} \Delta q(\mathbf{R}_{ij}), \\ (V_{\pm 2}^j)' &= \alpha f_{\pm 2}(\mathbf{R}_j) \\ &\equiv \alpha e \sum_{i=1}^n \frac{3(X_{ij}^2 - Y_{ij}^2 \pm 2iX_{ij}Y_{ij})}{R_{ij}^2} \Delta q(\mathbf{R}_{ij}). \end{aligned}$$

¹¹ T. J. Rowland, Phys. Rev. **125**, 459 (1962).

¹² G. M. Volkoff, Can. J. Phys. **31**, 820 (1953).

¹³ M. H. Cohen and F. Reif, in *Solid State Physics*, edited by F. Seitz and D. Turnbull (Academic Press Inc., New York, 1957), Vol. 5.

Here, eq is the EFG in the absence of screening, and Δq is given by

$$\Delta q(\mathbf{R}_{ij}) = (4A/3\pi R_{ij}^3) \cos(2k_F R_{ij} + \phi).$$

A and ϕ depend on partial-wave phase shifts and will be evaluated later. α is the enhancement factor of Kohn and Vosko and k_F is the Fermi wave number. Rotating into the magnetic field frame we have

$$\begin{aligned} |V_{\pm 1}^j|^2 &\approx 3 \sin^2 2\theta (f_{+2} + f_{-2}) \alpha eq \\ &\quad + \frac{1}{8} 3i \sin 4\theta (f_{+1} - f_{-1}) \alpha eq \\ &\quad + (9/16) \sin^2 2\theta (eq + \alpha f_0)^2, \end{aligned} \quad (4)$$

and

$$\begin{aligned} |V_{\pm 2}^j|^2 &\approx -\frac{3}{8} (1 + \cos^2 \theta) \sin^2 \theta (f_{+2} + f_{-2}) \alpha eq \\ &\quad + \frac{1}{8} 3i \sin^2 \theta \sin 2\theta (f_{+1} - f_{-1}) \alpha eq \\ &\quad + (9/16) \sin^4 \theta (eq + \alpha f_0)^2. \end{aligned} \quad (5)$$

We have neglected terms involving $(\alpha \Delta q)^2$. This approximation will be justified by the agreement obtained with the broadening data. Putting these expressions into (3) and averaging over all nuclear sites by using (1) we get

$$\begin{aligned} \bar{\nu} &= (1 + \bar{K}) \nu_R + \bar{a} \nu_R (3\mu^2 - 1) \\ &\quad + \frac{1}{2} [\bar{\nu}_Q^2 / \nu_R (1 + \bar{K})] (1 - 10\mu^2 + 9\mu^4). \end{aligned} \quad (6)$$

Here we get

$$\bar{\nu}_Q \equiv \frac{3e^2 Q}{2I(2I-1)\hbar} \left| q + \frac{\alpha c}{e} \sum_{\mathbf{R}'} f_0(\mathbf{R}) \right|, \quad (7)$$

$$\bar{K} \equiv K_0 - \frac{AK_0}{k_F^2} c \sum_{\mathbf{R}'} \frac{\sin(2k_F R + \phi)}{R^2}, \quad (8)$$

$$\begin{aligned} \bar{a} &\equiv a_0 + \frac{8\pi\beta^2 V_0 N(E_F) A}{3k_F^2} \alpha' c \\ &\quad \times \sum_{\mathbf{R}'} \frac{(3Z^2 - R^2)}{R^4} \sin(2k_F R + \phi), \end{aligned} \quad (9)$$

where β is the Bohr magneton, V_0 is the atomic volume, $N(E_F)$ is the density of states at the Fermi surface, and α' is an enhancement factor similar to α and approximately equal to it. α' is given by

$$\alpha' \equiv \frac{\int [u_{k_F}^2(\mathbf{r}') e^{2ik_F \cdot \mathbf{r}'} P_2(\cos \theta') r'^{-3}] d^3 r'}{\int [e^{2ik_F \cdot \mathbf{r}'} P_2(\cos \theta') r'^{-3}] d^3 r'}.$$

Equation (6) is identical with the corresponding expression obtained for pure indium,^{9,10} with all quantities given as mean values. Hence the powder-pattern singularity expressions are those given in Sec. II, and the Knight shifts and quadrupole coupling obtained from experiment are mean values as defined above.

We can now write the contribution of screening to linewidth broadening. For the $\frac{1}{2} \rightarrow -\frac{1}{2}$ transition, we

get, from (2) and (3),

$$\begin{aligned} \langle \delta^2 \nu \rangle_{\text{av}} = & c(1-c) \nu_R^2 \sum_{\mathbf{R}'} \{ \Delta K(\mathbf{R}) + \Delta a(\mathbf{R})(3\mu^2 - 1) \\ & + \alpha(\nu_q/\nu_0)^2 [-(1+8\mu^2-9\mu^4)(f_{+2}+f_{-2})/eq \\ & + 2i\mu(1-\mu^2)^{1/2}(5-9\mu^2)(f_{+1}-f_{-1})/eq \\ & + 3(1-10\mu^2+9\mu^4)(f_0/eq)] \}^2. \end{aligned} \quad (10)$$

Here, $\Delta K(\mathbf{R})$ and $\Delta a(\mathbf{R})$ are defined consistently with Eqs. (1), (6), and (7). For the 90° singularity (ν_H) one inserts $\mu=0$, and for the non- 90° singularity (ν_L) one inserts $\mu^2=(5/9)-(a\nu_R\nu_0/9\nu_q^2)$. For the 90° singularity ($\nu_{3/2}$) corresponding to the $\frac{3}{2} \rightarrow \frac{1}{2}$ transition we get

$$\begin{aligned} \langle \delta^2 \nu_{3/2} \rangle_{\text{av}} = & c(1-c) \nu_R^2 \sum_{\mathbf{R}'} \left[\Delta K(\mathbf{R}) - \Delta a(\mathbf{R}) \right. \\ & + \alpha \left(\frac{\nu_q(f_0+f_{+2}+f_{-2})}{\nu_0 2eq} \right) \\ & \left. + \frac{7\alpha}{8} \left(\frac{\nu_q}{\nu_0} \right)^2 \left(\frac{3f_0-f_{+2}-f_{-2}}{eq} \right) \right]^2. \end{aligned} \quad (11)$$

The experimentally determined Gaussian linewidths for the three singularities σ_H , σ_L , and $\sigma_{3/2}$ exhibit the effects of dipolar broadening as well as the broadening due to screening. Experimental values are given in Table I. In order to obtain quantities which depend on screening only, we assume with Rowland¹¹ that the second moments due to the two mechanisms are additive. The difference between second moments will then be due to screening only. Thus one obtains

$$\sigma_L^2 - \sigma_H^2 = \langle \delta^2 \nu_L \rangle_{\text{av}} - \langle \delta^2 \nu_H \rangle_{\text{av}}, \quad (12)$$

$$\sigma_{3/2}^2 - \sigma_H^2 = \langle \delta^2 \nu_{3/2} \rangle_{\text{av}} - \langle \delta^2 \nu_H \rangle_{\text{av}}, \quad (13)$$

where the right-hand sides of (12) and (13) are calculated from (10) and (11).

The enhancement factor α is regarded as a parameter to be obtained by fit to the data. The partial-wave phase shifts and screening parameters A and ϕ were obtained, as in Ref. 11, from the Blatt corrected Friedel sum rule and the residual resistivity of the alloys, and are to be found in Table II. Lattice parameter measurements were corrected to helium temperature using the measurements made on pure indium at that temperature by Barrett and quoted by Hewitt and Taylor.¹⁴ It is found that the sums in (10) and (11) must be truncated to exclude nearest-neighbor sites. α must be of the order of 100 to explain the broadening. Putting this value into (4), (5), and (3) yields a nearest-neighbor perturbation due to screening of about 200 kHz or more which carries the nuclei outside of the observed resonance. Moreover, no consistent, smaller, value of α can be obtained for all alloy systems if the nearest neighbors are retained. With this truncation, a value of α , 85 ± 15 , was found

¹⁴ R. R. Hewitt and T. T. Taylor, Phys. Rev. **125**, 524 (1962).

TABLE I. In^{115} Gaussian linewidth parameters in kHz for In-Cd, In-Hg, In-Tl, In-Sn, and In-Pb.

Solute	at. %	σ_H	σ_L	$\sigma_{3/2}$
Cd	0.20	28.7	24.8	26.6
	0.40	31.4	36.3	34.9
	0.61	36.3	32.2	37.0
	0.81	43.0	40.5	44.5
	1.02	34.0	39.0	37.4
	1.54	42.4	47.6	57.7
	2.06	43.3	60.0	74.1
	2.59	51.0	74.0	89.4
	3.13	54.6	67.5	108.6
	3.67	58.2	75.7	114.1
Hg	4.21	53.0	78.2	143.7
	4.76	50.3	90.4	158.8
	0.17	30.0	28.9	30.6
	0.28	29.2	30.2	33.6
	0.40	30.4	32.9	34.9
	0.57	31.7	31.0	35.5
	0.80	30.3	36.1	41.8
	1.64	32.8	40.8	47.2
	2.49	34.9	58.0	55.2
	3.37	43.0	60.8	75.2
Tl	4.28	43.9	58.0	106.7
	0.22	28.6	28.1	28.8
	0.39	31.3	33.1	34.2
	0.62	30.8	31.3	31.8
	0.79	32.7	30.4	37.2
	1.02	31.5	31.8	38.3
	1.55	30.7	37.8	49.5
	2.08	38.9	42.2	47.7
	2.57	35.7	53.4	50.0
	3.12	43.2	48.8	69.5
Sn	4.27	44.6	57.8	88.3
	5.45	40.9	62.2	91.2
	6.62	43.4	63.5	112.0
	0.19	35.3	34.9	40.3
	0.39	37.2	32.3	36.6
	0.58	41.4	40.8	42.2
	0.77	37.6	35.8	37.9
	0.97	42.4	42.0	42.2
	1.93	36.8	49.2	54.7
	2.90	43.7	59.3	58.5
Pb	3.87	46.6	68.9	67.7
	4.84	47.2	68.2	73.2
	5.81	50.9	71.4	81.9
	6.78	58.7	67.1	88.1
	7.56	50.9	74.9	84.1
	7.76	48.2	69.7	98.2
	7.94	59.8	89.7	103.2
	8.73	56.5	80.6	94.2
	9.70	56.0	90.9	101.1
	0.11	42.5	37.6	42.1
In	0.22	36.8	36.6	36.9
	0.33	44.1	38.5	39.3
	0.44	42.2	38.3	41.9
	0.56	36.0	39.3	45.9
	1.11	40.8	45.6	60.3
	1.68	45.9	58.8	61.4
	2.26	44.7	51.0	57.0
	2.83	55.9	50.7	68.6
	3.41	51.1	55.3	79.4
	4.00	47.9	68.2	83.1
	4.83	57.7	75.4	106.8
	5.80	66.3	94.0	123.2
In	100.00	42.9	36.5	32.3

to fit the broadening data of all five alloy systems. The experimental results for In-Sn and calculations for two values of α are shown in Figs. 1 and 2. The good fit to

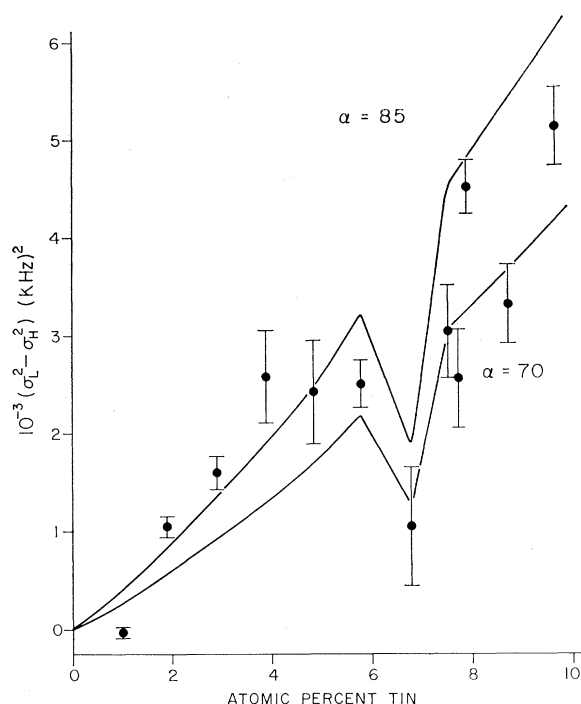


FIG. 1. Relative In^{115} single-crystal second moments for 90° and non- 90° crystallites. $\frac{3}{2} \rightarrow \frac{1}{2}$ transition in In-Sn.

10 at. % Sn supports the conclusion that the assumptions and approximations made were good ones. The predicted and observed dip seen in Fig. 1 is a lattice parameter effect associated with the oscillation of the lattice parameters in the neighborhood of 7 at. % Sn. The line broadening is dominated by the quadrupolar interactions. Using Eqs. (4) and (5) we were able to compute line shapes taking into account 538 nearest neighbors. An example of this calculation is shown in Fig. 3 for In-0.6 at. % Cd for various values of dipolar broadening. As expected from the observed powder-pattern line shapes, we obtain a strong Gaussian central peak. The weak asymmetric wings could not be observed, but they make the mean frequency different from the observed peak frequency. As explained previously, the mean frequencies are needed for the perturbation expressions. However, the difference is small for values of the dipolar broadening corresponding to indium (≈ 30 kHz). The worst case, the $\frac{3}{2} \rightarrow \frac{1}{2}$ singu-

TABLE II. Blatt corrected valence difference Z' , residual resistivity ρ in $\mu\Omega$ cm/at. %, phase shifts, and screening parameters, with $\eta_2 = 0.11\eta_1$.

Solute	Z'	ρ	η_0	η_1	A	ϕ
Sn	0.892	0.376	0.738	0.187	0.355	-1.721
Pb	0.481	0.600	0.756	0.000	0.686	-2.386
Cd	-0.773	0.325	-0.674	-0.152	0.344	-1.209
Hg	-0.681	0.114	-0.356	-0.238	0.364	3.016
Tl	-0.261	0.197	-0.410	0.000	0.399	-0.410

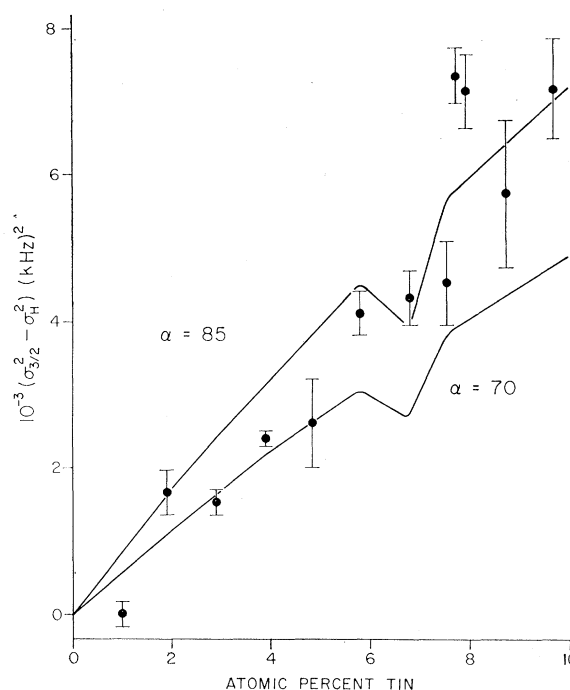


FIG. 2. Relative In^{115} single-crystal second moments for $\frac{3}{2} \rightarrow \frac{1}{2}$ and $\frac{1}{2} \rightarrow -\frac{1}{2}$ transitions in 90° crystallites of In-Sn.

larity of In-Sn, is shown in Fig. 4. Even here the difference between peak and mean frequencies is an order of magnitude too small to explain the dip in the Knight shift observed in that alloy. Moreover, the difference has only a monotonic behavior with concentration of solute and would not be able to exhibit the dip even if the effect were large enough.

IV. KNIGHT SHIFT AND QUADROPOLAR-COUPLING RESULTS

The measured isotropic and anisotropic Knight shifts in In-Cd, In-Hg, and In-Tl are shown in Figs. 5-10. As

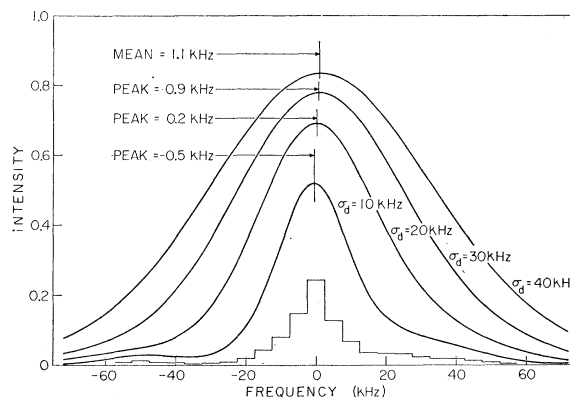


FIG. 3. Calculated full-power curve for In -0.6 at. % Cd, with and without spin-spin broadening. Strength of imposed Gaussian broadening is indicated by σ_d .

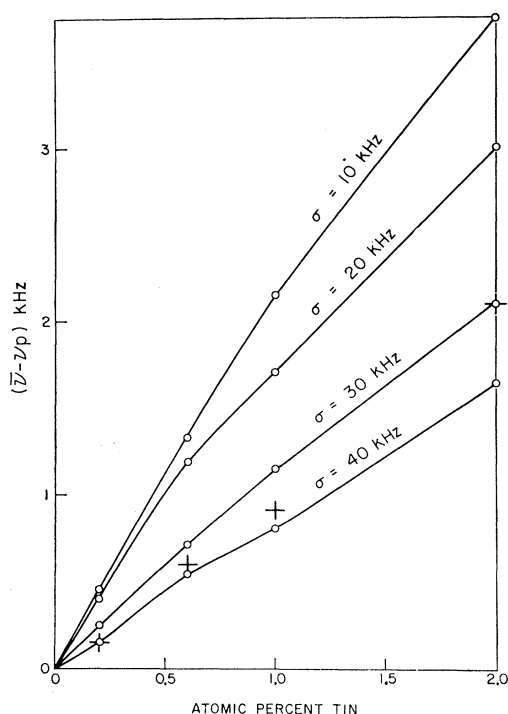


FIG. 4. Difference between mean and peak frequencies for $\frac{3}{2} \rightarrow \frac{1}{2}$ transition in In-Sn, for several values of the Gaussian broadening width parameter σ . Crosses indicate value of σ deduced from experiment.

was the case in the In-Sn and In-Pb alloys,⁵ the isotropic Knight shift shows a rapid drop in the dilute region. This drop is two orders of magnitude larger than predicted by the screening term in Eq. (8). The increase in the isotropic Knight shift after 2 at.% Cd is similar in nature to that observed after 7 at.% Sn in In-Sn.⁵ Both alloys demonstrate an oscillation in lattice parameters which has been ascribed to the approach, intersection, and overlap of the Fermi surface with a Brillouin-zone face.^{15,16} Such a process would be expected to lead to an increase in the density of states at

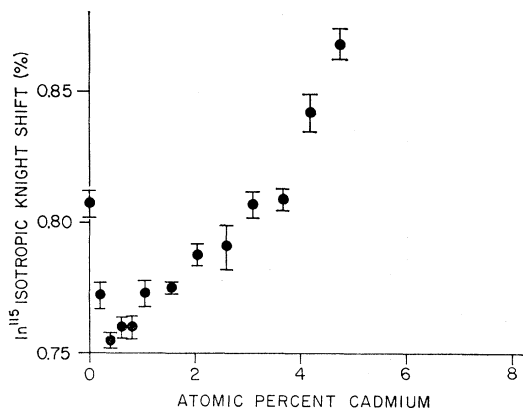


FIG. 5. ^{115}In isotropic Knight shift in In-Cd.

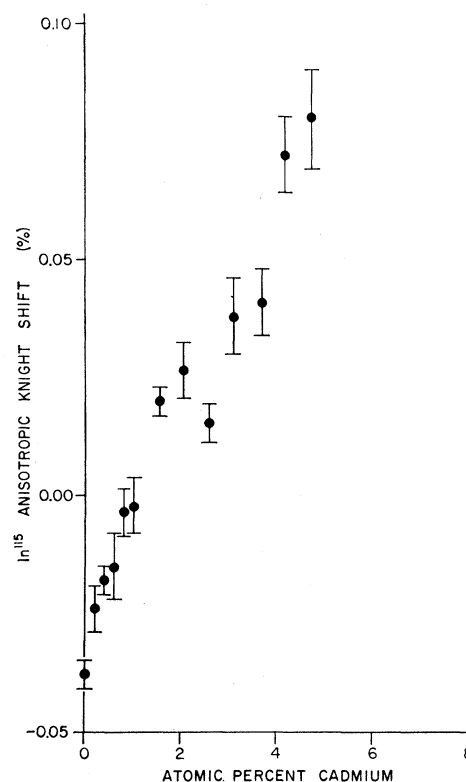


FIG. 6. ^{115}In anisotropic Knight shift in In-Cd.

the Fermi surface, and hence to an increase in the Knight shifts.

The anisotropic Knight shifts in the alloys behave as previously observed in In-Sn and In-Pb, a roughly linear increase with impurity concentration. The screening term in Eq. (9), calculated with an $\alpha' = 85$, is an order of magnitude too small to describe the observed changes.

The measured quadrupole-coupling frequencies in In-Cd, In-Hg, and In-Tl are shown in Figs. 11 and 12. The quadrupole-coupling frequency in the alloys is given by Eq. (7). The contribution of the lattice and the unperturbed Bloch electrons, denoted by q , should depend only on the lattice parameters of the alloy at

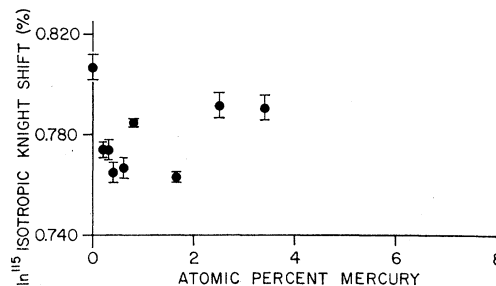
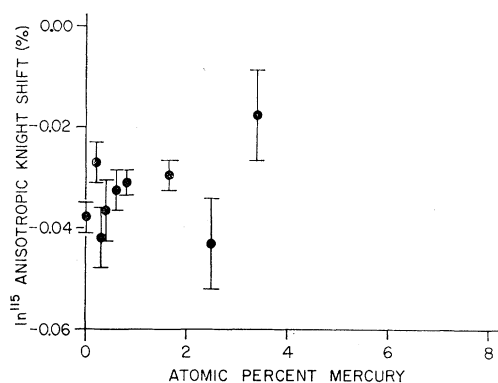
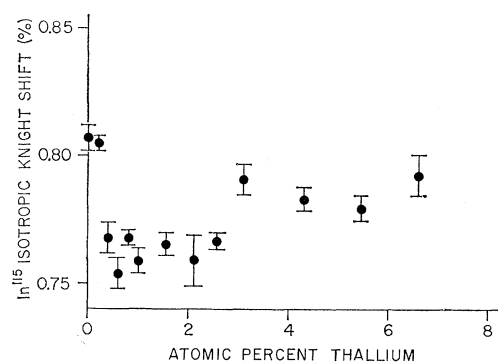


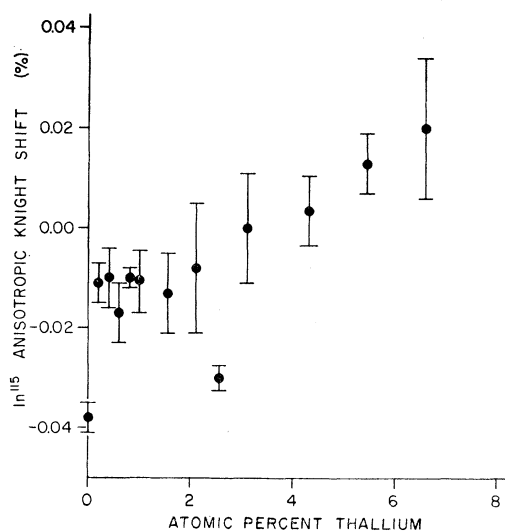
FIG. 7. ^{115}In isotropic Knight shift in In-Hg.

¹⁵ M. F. Merriam, Phys. Rev. Letters **11**, 321 (1963).

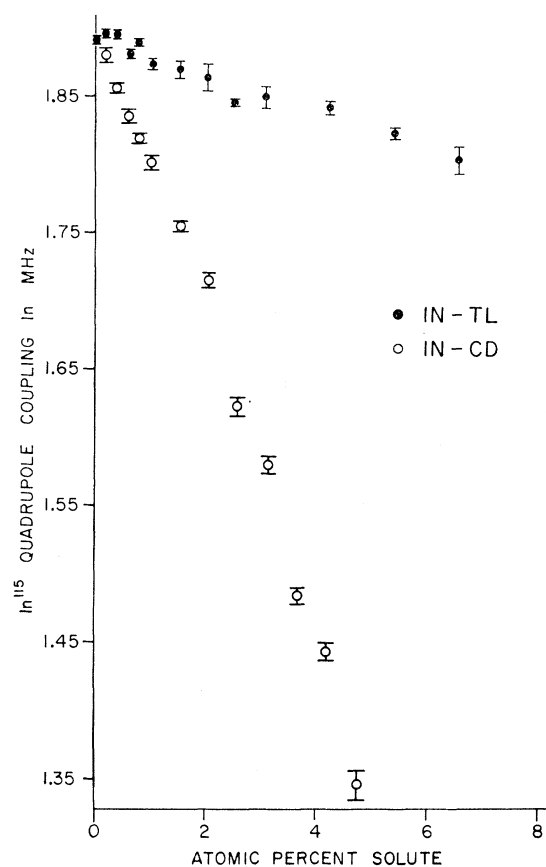
¹⁶ M. F. Merriam, Phys. Rev. **144**, 300 (1966).

FIG. 8. In^{115} anisotropic Knight shift in In-Hg.FIG. 9. In^{115} isotropic Knight shift in In-Tl.

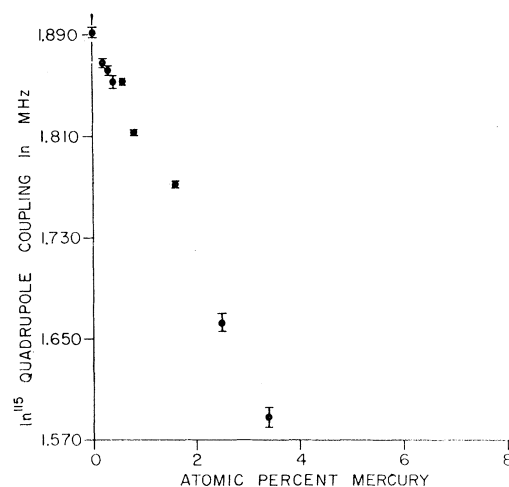
constant temperature. Examination of Figs. 11 and 12 and the corresponding measurements of Anderson *et al.*⁵ on In-Sn and In-Pb, reveals a one-to-one correspondence between the c/a ratio of the bct lattice and the quadrupole-coupling frequency. This is consistent with the pressure work of O'Sullivan and Schirber,¹⁷ who

FIG. 10. In^{115} anisotropic Knight shift in In-Tl.

¹⁷ W. J. O'Sullivan and J. E. Schirber, Phys. Rev. **135**, A1261 (1964).

FIG. 11. In^{115} quadrupole-coupling frequency in In-Cd and In-Tl.

found a strong dependence of the coupling on c/a ratio and a weak dependence on volume. The quadrupole-coupling frequency is plotted versus c/a ratio in five indium-rich alloys in Fig. 13. The strong dependence on c/a ratio is clear. Since the sign of the nuclear quad-

FIG. 12. In^{115} quadrupole-coupling frequency in In-Hg.

quadrupole moment is known we can write q as

$$q = \pm 0.5935 \nu_q - \frac{\alpha c}{e} \sum_{\mathbf{R}}' f_0(\mathbf{R}),$$

where q is in units of 10^{24} cm^{-3} and ν_q is in MHz. We emphasize that q is not explicitly dependent on the particular impurity in the alloy, but depends only on the c/a ratio and the atomic volume. We anticipate a $1/V$ dependence on atomic volume. The quantity Vq should depend only on the c/a ratio and is plotted in Fig. 14 for the assumption of a positive EFG and in Fig. 15 for a negative EFG. Examination of these figures shows quite clearly that EFG in indium is negative. Accepting Sternheimer's value for the antishielding factor in indium¹⁸ and using the ionic model of Hewitt and Taylor,¹⁴ we obtain for the electronic contribution to the EFG, -390.7×10^{12} (cgs-esu).

The rate of change of the EFG with respect to the c/a ratio is 70% of that obtained by O'Sullivan and Schirber¹⁷ at room temperature.

V. CONCLUSION

The dip in the isotropic Knight shift observed for low concentrations of impurities in indium-rich alloys is the most surprising, and perhaps the most interesting,

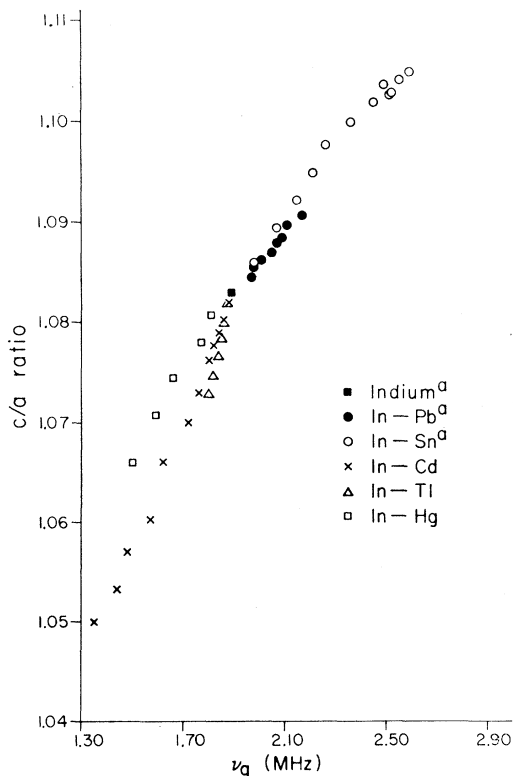


FIG. 13. ^{115}In quadrupole-coupling frequency versus c/a ratio in five indium-rich alloys. (a) From Ref. 5.

¹⁸ R. M. Sternheimer, Phys. Rev. **159**, 266 (1967).

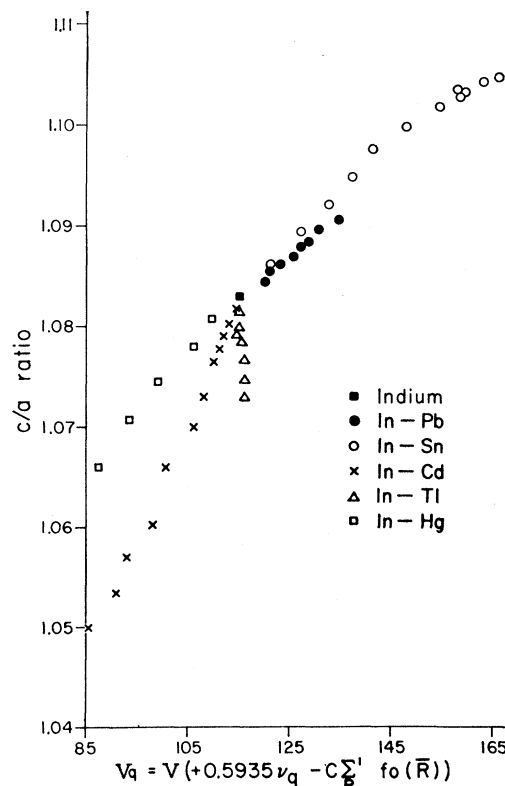


FIG. 14. Dimensionless quantity Vq in five indium-rich alloys for positive EFG.

result of the NMR measurements on these alloys. In view of the fact that the dip is observed for alloys with different trends in c/a ratio, atomic volume, and electrons/atom, an explanation based on a change in the nearly free-electron band structure is implausible. Recent density of states calculations for solid indium¹⁹ indicate very smooth behavior in the neighborhood of the Fermi energy, so that the addition of a fraction of an atomic percent impurity would not be expected to yield a significant drop in the density of states. Moreover, electronic specific-heat measurements below 1 at.% Sn in In-Sn²⁰ do not show a dip similar to that observed in the isotropic Knight shift.

Differences between the alloy systems studied lie principally in the rate at which the Knight shift drops with impurity concentration, decreasing most rapidly for In-Pb. If one plots the measured Knight shifts versus residual resistivity, one finds that the rate at which the Knight shift drops is the same for all five alloy systems. This indicates that the drop is related to the scattering of Fermi electrons by the impurities.

The screening theory explains the linewidth and quadrupole-coupling results quite well, but does not explain the Knight shift results at all. This leads us to

¹⁹ R. W. Shaw, Jr., and N. V. Smith, Phys. Rev. **178**, 985 (1969).

²⁰ H. W. White and D. C. McCollum, Bull. Am. Phys. Soc. **13**, 1671 (1968).

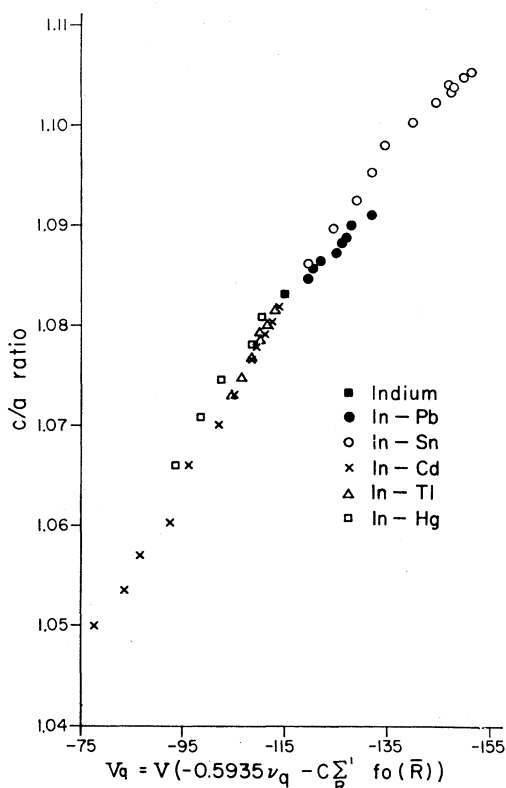


FIG. 15. Dimensionless quantity Vq in five indium-rich alloys for negative EFG.

believe that the spin susceptibility of the conduction-electron system is decreasing, initially, as a result of the scattering of Fermi electrons by the impurities. The corresponding increase in the negative anisotropic Knight shift would be too small for us to detect. The anisotropic Knight shift behavior can be understood in terms of the changing orbital character of the Bloch electrons.

The question remains as to what is producing a decrease in spin susceptibility. We note that reduction of electron-electron interactions has been cited as the reason for the initial drop in the superconducting transition temperature in indium alloys.²¹ In this case, reduction of the anisotropy of the electron-phonon interaction, produced by impurity scattering of Fermi electrons, is responsible for a drop in the superconduct-

ing transition temperature. Repulsive electron-electron interactions are known to enhance the spin susceptibility relative to its independent particle value. Work on the exchange enhancement of the susceptibility in alkali and noble metals indicates that the enhancement is substantial.^{6,7} A quantitative theory has not yet been done for polyvalent metals, but the qualitative conclusions should be the same. We suggest, therefore, that the drop in the Knight shift may be due to a reduction of repulsive electron-electron interactions, possibly through a loss of anisotropy as a result of impurity scattering of Fermi electrons.

There is further evidence that electron-electron interactions are responsible for the isotropic Knight shift behavior. Short-range exchange interactions lead to an enhancement in the nuclear spin-lattice relaxation rate.^{6,7} MacLaughlin²² has observed a dip in the relaxation rate of In-Pb alloys in the dilute region at 4.2°K. MacLaughlin's preliminary results indicate that the Korringa product K^2T_1T is not constant. This is consistent with a changing electron-electron interaction.

It is not clear why the isotropic Knight shift rises again to near its pure indium value in a number of the alloys. A number of effects, including band structure, may be involved. A full explanation of the Knight shift behavior, including the higher concentrations, may have to invoke the suggestion of Bennett *et al.*²³ that the product of the hyperfine field with the spin susceptibility must be calculated for each segment of the Fermi surface, with a summation over segments.

The screening theory of Kohn and Vosko explains the broadening of the indium lines well. The value of 85 ± 15 for the enhancement factor obtained from the width analysis is consistent with enhancement factors obtained in other metals, 40 in both copper²⁴ and silver.²⁵ The stronger lattice potential of a polyvalent metal should yield a larger α than is obtained in the previously measured monovalent metals.

ACKNOWLEDGMENTS

The authors thank Dr. W. T. Anderson for making the In-Sn and In-Pb width data available for use. We also thank Dr. D. MacLaughlin for permitting us to mention his unpublished work on indium alloys.

²² D. E. MacLaughlin (unpublished).

²³ L. H. Bennett, R. W. Mebs, and R. E. Watson, *Phys. Rev.* **171**, 611 (1968).

²⁴ T. J. Rowland, *Phys. Rev.* **119**, 900 (1960).

²⁵ G. W. Hinman, G. R. Hoy, J. K. Lees, and J. C. Serio, *Phys. Rev.* **135**, A206 (1964).

²¹ D. Markowitz and L. P. Kadanoff, *Phys. Rev.* **131**, 563 (1963).